INVITED PAPER *Special Section on Signal Design and its Application in Communications*

Recent Advances in Single-Carrier Frequency-Domain Equalization and Distributed Antenna Network

Fumiyuki ADACHI[†a)], ***Fellow***, **Kazuki TAKEDA**[†], **Tatsunori OBARA**[†], **Tetsuya YAMAMOTO**[†], ***and*** **Hiroki MATSUDA**[†], ***Student Members***

SUMMARY Broadband wireless technology that enables a variety of gigabit-per-second class data services is a requirement in future wireless communication systems. Broadband wireless channels become extremely frequency-selective and cause severe inter-symbol interference (ISI). Furthermore, the average received signal power changes in a random manner because of the shadowing and distance-dependant path losses resulted from the movement of a mobile terminal (MT). Accordingly, the transmission performance severely degrades. To overcome the performance degradation, two most promising approaches are the frequency-domain equalization (FDE) and distributed antenna network (DAN). The former takes advantage of channel frequency-selectivity to obtain the frequency-diversity gain. In DAN, a group of distributed antennas serve each user to mitigate the negative impact of shadowing and path losses. This article will introduce the recent advances in FDE and DAN for the broadband single-carrier (SC) transmissions.

key words: *single -carrier, frequency-domain equalization, distributed antenna network, MIMO, signal detection*

1. Introduction

The future wireless communications systems are expected to offer a variety of broadband data services of close to or even above 1 Gbps [1]. However, for such broadband data services, channels become extremely frequency-selective and cause severe inter-symbol interference (ISI), thereby severely degrading the bit error rate (BER) performance [2]. The use of an advanced equalization technique is indispensable. In general, there are two types of signal transmission: multi-carrier (MC) and single-carrier (SC). An advantage of SC signal transmissions over MC is its lower peak-to-average power ratio (PAPR). This lower PAPR property of SC is quite beneficial for the uplink (terminal-to-base) transmissions.

As for SC equalization, simple one-tap frequency-domain equalization (FDE) has been extensively studied [3]–[7]. Although the one-tap FDE can exploit the channel frequency-selectivity to improve the BER performance, its performance improvement is limited due to the residual ISI after FDE. Recently, we proposed a new frequency-domain block signal detection that incorporates the idea of multi-input/multi-output (MIMO) signal detection into FDE to effectively suppress the ISI [8].

Manuscript received February 12, 2010.
Manuscript revised June 6, 2010.

[†]The authors are with the Dept. of Electrical and Communication Engineering, Graduate School of Engineering, Tohoku University, Sendai-shi, 980-8579 Japan.
a) E-mail: adachi@ecei.tohoku.ac.jp

DOI: 10.1587/transfun.E93.A.2201

In addition to the ISI problem of broadband SC signal transmissions, the shadowing and distance-dependent path losses cause a severe power loss problem since the transmit power is limited. The power loss problem is a crucial issue as well as the ISI problem in order to make the frequency and power efficient broadband wireless communication systems a reality. Distributed antenna system or network (DAS or DAN) [9]–[14] can solve the power loss problem. In DAN, many antennas are spatially distributed over a coverage area of a DAN signal processing center (SPC), which takes the role of conventional base station (BS). There are always some distributed antennas in the vicinity of a mobile terminal (MT) and they can cooperate to perform spatial diversity, beam forming, or spatial multiplexing. Since different antennas are located at different positions, DAN can exploit the random variations in the shadowing and path losses. We have been investigating the potential of DAN downlink spatial diversity using maximal-ratio transmission (MRT) [14].

This article will introduce the recent advances in FDE and DAN for the broadband SC signal transmissions.

2. Broadband Wireless Channel

The broadband fading channel model is illustrated in Fig. 1. There are several large obstacles between a BS and an MT and also many local scatterers (such as neighboring buildings) in the vicinity of the MT. The reflection of the signal by large obstacles creates the propagation paths with different time delays; each path is a cluster of irresolvable multipaths created by reflection or diffraction, by local scatterers, of the transmitted signal reaching the surroundings of the

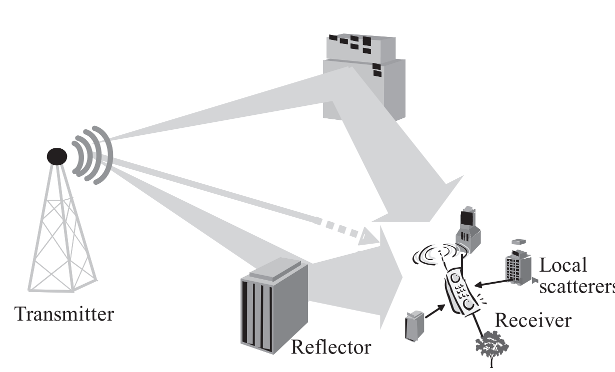

Fig. 1 Fading channel model.

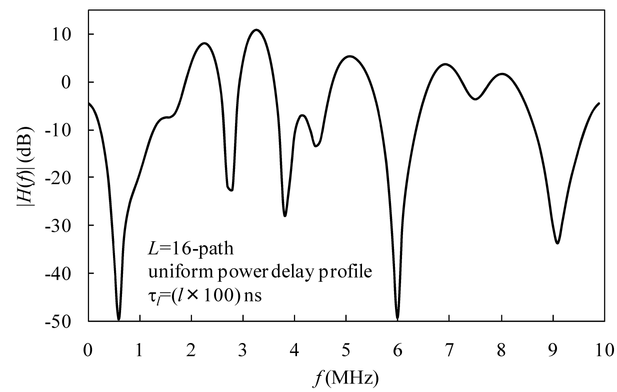

Fig. 2 Frequency-selective channel.

MT.

The SC signal transmission with FDE is a block transmission. The channel transfer function severely changes both in the frequency- and time-domains according to the movement of an MT. However, the channel can be assumed to stay constant during the transmission of one block, so that, the time-selectivity can be neglected. Assuming a symbol-spaced L-path channel, the channel impulse response $h(\tau)$ can be expressed as [15]

$$h(\tau) = \sum_{l=0}^{L-1} h_l \delta(\tau - \tau_l), \tag{1}$$

where h_l and τ_l are the complex-valued path gain with $E\left[\sum_{l=0}^{L-1} |h_l|^2\right] = 1$ ($E[.]$ denotes the expectation operation) and time delay of the lth path, respectively.

The channel transfer function (or the channel gain at frequency f) is the Fourier transform of $h(\tau)$ and is given by

$$H(f) = \sum_{l=0}^{L-1} h_l \exp(-j2\pi f \tau_l). \tag{2}$$

When $H(f)$ changes within the signal bandwidth, the channel is called the frequency-selective channel. A one shot observation of $H(f)$ is illustrated in Fig. 2. A frequency-selective channel having an $L = 16$-path uniform power delay profile with $E[|h_l|^2] = 1/L$ and $\tau_l = l \times 100$ ns (i.e., the l-th path length is $l \times 30$ m) is assumed. The frequency-selective channel severely distorts the received SC signal spectrum and thus, the use of advanced equalization techniques is indispensable [2].

3. Channel Capacity

The channel capacity analysis for broadband SC transmissions is an interesting study topic. In [16], the achievable channel capacity of broadband SC signal transmissions with FDE in a frequency-selective channel is theoretically examined and compared to that of orthogonal frequency division multiplexing (OFDM). It is shown [16] that the OFDM with adaptive modulation provides always higher channel capacity than SC using one-tap FDE. However, below we will show that when block signal detection is utilized, the broadband SC transmission has a potential to achieve the same channel capacity as OFDM.

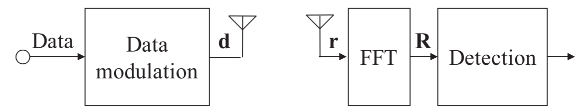

Fig. 3 SC signal transmission system model.

The SC signal transmission system model is illustrated in Fig. 3 (in this paper, for the simplicity purpose, we omit the insertion and removal of cyclic prefix (CP)). An N_c-symbol block $\boldsymbol{d} = [d(0), \cdots, d(t), \cdots, d(N_c - 1)]^T$ is transmitted over a frequency-selective channel. The received signal block $\boldsymbol{r} = [r(0), \cdots, r(t), \cdots, r(N_c - 1)]^T$ can be expressed in the matrix form as

$$\boldsymbol{r} = \sqrt{\frac{2E_s}{T_s}} \boldsymbol{hd} + \boldsymbol{n}, \tag{3}$$

where E_s and T_s are respectively the data-modulated symbol energy and length, $\boldsymbol{h}$ is the channel impulse response matrix given as

$$\boldsymbol{h} = \begin{bmatrix} h_0 & & & & h_{L-1} & \cdots & h_1 \\ h_1 & \ddots & & & & \ddots & \vdots \\ \vdots & \ddots & h_0 & & \boldsymbol{0} & & h_{L-1} \\ h_{L-1} & & h_1 & \ddots & & & \\ & \ddots & \vdots & \ddots & \ddots & & \\ & & h_{L-1} & & \ddots & h_0 & \\ & & & \ddots & & h_1 & \ddots \\ \boldsymbol{0} & & & & \ddots & \vdots & \ddots & h_0 \end{bmatrix}, \tag{4}$$

and $\boldsymbol{n} = [n(0), \cdots, n(t), \cdots, n(N_c - 1)]^T$ is the noise vector. The frequency-domain representation $\boldsymbol{R} = [R(0), \cdots, R(k), \cdots, R(N_c-1)]^T$ of the received signal block is given as

$$\boldsymbol{R} = \boldsymbol{Fr} = \sqrt{\frac{2E_s}{T_s}} \boldsymbol{HFd} + \boldsymbol{N}, \tag{5}$$

where $\boldsymbol{H} = \boldsymbol{FhF}^H$ and $\boldsymbol{N} = \boldsymbol{Fn}$ with $[.]^H$ denoting the Hermitian transpose operation and $\boldsymbol{F}$ being an $N_c \times N_c$ fast Fourier transform (FFT) matrix given by

$$\boldsymbol{F} = \frac{1}{\sqrt{N_c}} \begin{bmatrix} 1 & 1 & \cdots & 1 \\ 1 & e^{-j2\pi\frac{1\times1}{N_c}} & \cdots & e^{-j2\pi\frac{1\times(N_c-1)}{N_c}} \\ \vdots & \vdots & \ddots & \vdots \\ 1 & e^{-j2\pi\frac{(N_c-1)\times1}{N_c}} & \cdots & e^{-j2\pi\frac{(N_c-1)\times(N_c-1)}{N_c}} \end{bmatrix}. \tag{6}$$

$\boldsymbol{H}$ is the channel matrix, which is diagonal because of the circulant property of $\boldsymbol{h}$, and is given by

$$\boldsymbol{H} = \boldsymbol{F}\boldsymbol{h}\boldsymbol{F}^H = \begin{bmatrix} H(0) & & & & \\ & \ddots & & \mathbf{0} & \\ & & H(k) & & \\ & \mathbf{0} & & \ddots & \\ & & & & H(N_c-1) \end{bmatrix}. \quad (7)$$

Equation (5) implies that the SC frequency-domain received signal has the same signal representation as an $N_c \times N_c$ MIMO multiplexing with channel matrix $\boldsymbol{HF}$ but with a symbol rate per stream reduced by a factor of N_c. Following [17], the channel capacity C of SC signal transmission is given as

$$\begin{aligned} C &= \frac{1}{N_c}\log_2 \det\left(\boldsymbol{I} + \frac{E_s}{N_0}(\boldsymbol{HF})(\boldsymbol{HF})^H\right) \\ &= \frac{1}{N_c}\sum_{k=0}^{N_c-1}\log_2\left(1 + \frac{E_s}{N_0}|H(k)|^2\right), \end{aligned} \quad (8)$$

which is identical to the channel capacity of OFDM with N_c subcarriers [18].

4. Frequency-Domain Block Signal Detection

The frequency-domain received signal representation is given by Eq. (5). The task of the receiver is to estimate the transmit signal block $\boldsymbol{d}$ for the given received signal $\boldsymbol{R}$. Recently, we proposed a new SC signal detection, called frequency-domain block signal detection, based on the frequency-domain received signal representation given by Eq. (5) [8]. The conceptual structure of SC transmission using frequency-domain block signal detection is illustrated in Fig. 4.

We incorporate an iterative frequency-domain successive interference cancellation & minimum mean square error detection (iterative FD-SIC&MMSED) and frequency-domain maximum likelihood detection (MLD) employing QR decomposition/M-algorithm (FD-QRM-MLD), which are modified versions of the Vertical-Bell Laboratories layered space-time architecture (V-BLAST) detection [19] and the QRM-MLD [20], respectively, developed for the signal detection for MIMO multiplexing. The QRM-MLD is known to achieve the BER performance fairly close to the MLD but with quite reduced complexity. The algorithms of iterative FD-SIC&MMSED and FD-QRM-MLD are illustrated in Fig. 5.

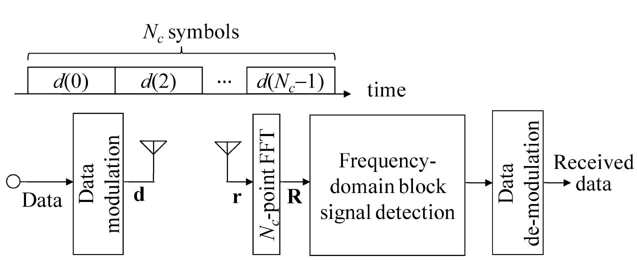

Fig. 4 Conceptual structure of SC transmission using frequency-domain block signal detection.

4.1 Iterative FD-SIC&MMSED

The frequency-domain block signal detection using iterative FD-SIC&MMSED can achieve better BER performance than the conventional one-tap FDE based on the MMSE criterion (MMSE-FDE).

The FD-SIC&MMSED is composed of i) ordering, ii) ISI cancellation, and iii) signal detection. The transmitted symbol which has the highest signal-to-interference plus noise power ratio (SINR) among undetected symbols is detected by performing MMSED [21]. However, in the case of SC transmission, since the SINR is the same for all symbols in a block, no ordering is necessary; the detection can be carried out simply from the first symbol (i.e., $d(0)$) in a block. The replicas of the symbols except for the one to be detected are generated and subtracted from the received signal (i.e., ISI cancellation). The MMSE weight matrix is updated for carrying out MMSED. Until all of the transmitted symbols are detected, the above interference cancellation and detection is repeated.

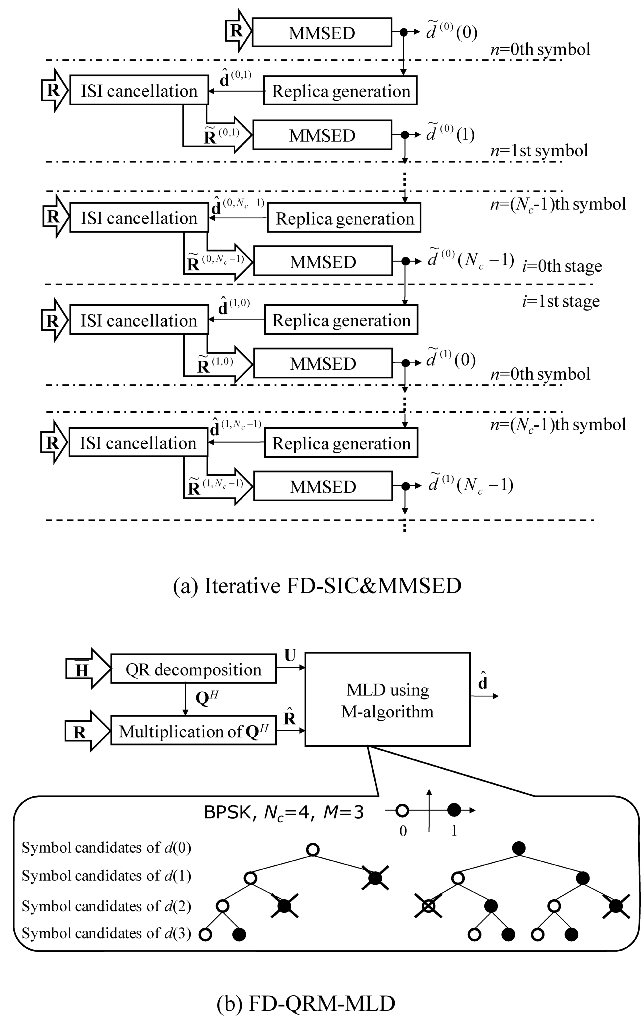

Fig. 5 Iterative FD-SIC&MMSED and FD-QRM-MLD.

The single use of FD-SIC&MMSED cannot suppress the ISI sufficiently, in particular for those symbols which have been detected earlier. To further improve the BER performance, iterative processing can be used [22]. After all of transmitted symbols are detected, the FD-SIC&MMSED is carried out again. This is repeated a sufficient number of times. Below, the detection of the nth symbol ($n = 0{\sim}N_c-1$) in the ith iteration stage is presented.

(1) ISI cancellation

The frequency-domain received signal vector $\tilde{\boldsymbol{R}}^{(i,n)}$ for the detection of the nth symbol in the ith iteration stage (note that the symbols with $n' = 0{\sim}n-1$ have been detected) is given by

$$\tilde{\boldsymbol{R}}^{(i,n)} = \boldsymbol{R} - \sqrt{\frac{2E_s}{T_s}}\bar{\boldsymbol{H}}\hat{\boldsymbol{d}}^{(i,n)}, \tag{9}$$

where $\bar{\boldsymbol{H}} = \boldsymbol{HF} = [\bar{\boldsymbol{H}}_0, \cdots, \bar{\boldsymbol{H}}_n, \cdots, \bar{\boldsymbol{H}}_{N_c-1}]$ and $\hat{\boldsymbol{d}}^{(i,n)} = [\hat{d}^{(i)}(0), \cdots, \hat{d}^{(i)}(n-1), 0, \hat{d}^{(i-1)}(n+1), \cdots, \hat{d}^{(i-1)}(N_c-1)]^T$ is the soft decision replica vector. The interference replicas $\{\bar{\boldsymbol{H}}_{n'}\hat{d}^{(i)}(n');\ n' = 0{\sim}n-1\}$ are generated using a sequence of the log likelihood ratios (LLRs) of the present iteration stage associated with $\{d(n');\ n' = 0{\sim}n-1\}$. The symbols with indices $n' = n{\sim}(N_c-1)$ are undetected and hence, their replicas are generated using LLRs of the previous iteration stage.

(2) Signal detection

The ISI still remains after ISI cancellation and therefore, the MMSE weight matrix needs to be updated taking into account the residual ISI. The MMSE weight matrix updating proposed in [23] can be applied.

The MMSE weight matrix taking into account the residual ISI for the detection of the nth symbol in the ith iteration stage is given by

$$\boldsymbol{W}^{(i,n)} = \bar{\boldsymbol{H}}_n^H\left[\bar{\boldsymbol{H}}\boldsymbol{\rho}^{(i,n)}\bar{\boldsymbol{H}}^H + \left(\frac{E_s}{N_0}\right)^{-1}\boldsymbol{I}\right]^{-1}, \tag{10}$$

where $\boldsymbol{\rho}^{(i,n)} = \mathrm{diag}[\rho_0^{(i)}, \cdots, \rho_{n'}^{(i)}, \cdots, \rho_{N_c-1}^{(i)}]$ with $\rho_{n'}^{(i)} = E[|d(n') - \hat{d}^{(i)}(n')|^2]$ representing the extent to which the ISI remains on the n'th symbol. In the case of quadrature phase shift keying (QPSK) data modulation, $\rho_{n'}^{(i)}$ is given as [24]

$$\rho_{n'}^{(i)} = \begin{cases} \dfrac{2e^{\lambda_{n'}^{(i)}(0)}}{\left(e^{\lambda_{n'}^{(i)}(0)}+1\right)^2} + \dfrac{2e^{\lambda_{n'}^{(i)}(1)}}{\left(e^{\lambda_{n'}^{(i)}(1)}+1\right)^2}, & \text{if } n' < n \\ 1, & \text{if } n' = n \\ \dfrac{2e^{\lambda_{n'}^{(i-1)}(0)}}{\left(e^{\lambda_{n'}^{(i-1)}(0)}+1\right)^2} + \dfrac{2e^{\lambda_{n'}^{(i-1)}(1)}}{\left(e^{\lambda_{n'}^{(i-1)}(1)}+1\right)^2}, & \text{if } n' > n \end{cases}, \tag{11}$$

where $\lambda_{n'}^{(i)}(x)$ is the log-likelihood ratio (LLR) of the xth bit in the n'th symbol ($x = 0{\sim}1$ and $n' = 0{\sim}N_c-1$) obtained in the ith iteration stage.

When $i = 0$, the symbols with $n' > n$ are undetected and hence, $\rho_{n'}^{(i)}$ is replaced by 1. After ISI cancellation using soft replicas as shown by Eq. (9), MMSE detection on the nth symbol is performed by multiplying the frequency-domain received signal vector $\tilde{\boldsymbol{R}}^{(i,n)}$ by $1 \times N_c$ MMSE weight matrix $\boldsymbol{W}^{(i,n)}$ as

$$\tilde{d}^{(i)}(n) = \boldsymbol{W}^{(i,n)}\tilde{\boldsymbol{R}}^{(i,n)}. \tag{12}$$

4.2 FD-QRM-MLD

In the case of SC transmissions, all symbols have the same SINR and hence, no ordering is necessary; signal detection can be carried out simply from the last symbol $d(N_c-1)$. $\bar{\boldsymbol{H}}$ is decomposed by using the QR decomposition as

$$\bar{\boldsymbol{H}} = \boldsymbol{QU}, \tag{13}$$

where $\boldsymbol{Q}$ is an $N_c \times N_c$ unitary matrix (i.e., $\boldsymbol{Q}^H\boldsymbol{Q} = \boldsymbol{I}$ with $\boldsymbol{I}$ representing the identity matrix) and $\boldsymbol{U}$ is an $N_c \times N_c$ upper triangular matrix given by

$$\boldsymbol{U} = \boldsymbol{Q}^H\bar{\boldsymbol{H}} = \begin{bmatrix} U_{0,0} & U_{0,1} & \cdots & U_{0,N_c-1} \\ & U_{1,1} & \cdots & U_{1,N_c-1} \\ & & \ddots & \vdots \\ \boldsymbol{0} & & & U_{N_c-1,N_c-1} \end{bmatrix}. \tag{14}$$

The transformed frequency-domain received signal $\hat{\boldsymbol{R}}$ is obtained as

$$\hat{\boldsymbol{R}} = \boldsymbol{Q}^H\boldsymbol{R} = \sqrt{\frac{2E_s}{T_s}}\boldsymbol{Ud} + \boldsymbol{Q}^H\boldsymbol{N}. \tag{15}$$

The M-algorithm [25] is composed of N_c stages with the nth stage corresponding to the (N_c-1-n)th symbol in a block ($n = 0{\sim}N_c-1$). In each stage, the branch metric defined as the squared Euclidian distance from $\hat{\boldsymbol{R}}$ is computed for all candidate symbols (4 symbols for QPSK and 16 symbols for 16QAM) connected to each of M surviving symbols in the previous stage and then, only a total of M symbols having the smallest accumulated branch metrics are selected as the surviving symbols in the present stage and others are discarded. This process is repeated until the last stage (i.e., the first symbol $d(0)$ in a block). Finally, the symbol which has the smallest accumulated branch metric is chosen and a sequence of N_c detected symbols is obtained by tracing back the surviving symbols until the first stage.

4.3 BER Performance

We assume a block transmission of $N_c = 64$ symbols, where two data modulation schemes, QPSK and 16QAM, are considered. The channel is assumed to be a frequency-selective block Rayleigh fading channel having symbol-spaced L = 16-path uniform power delay profile. Ideal channel estimation is assumed. The average BER performances of SC block signal detection using iterative FD-SIC&MMSED and FD-QRM-MLD are compared in Fig. 6 as a function of the average received signal energy per bit-to-noise power spectrum density ratio E_b/N_0. For FD-QRM-MLD, three

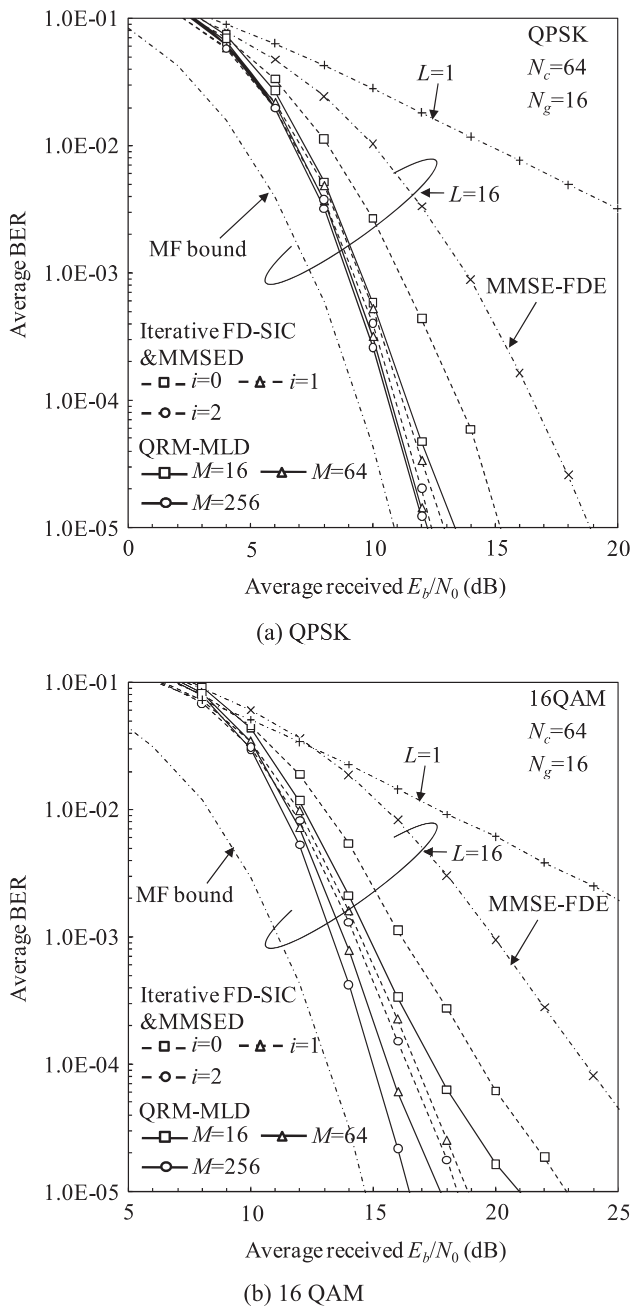

(a) QPSK

(b) 16 QAM

Fig. 6 BER performance of SC block signal detection.

cases of the number M of surviving symbols in each stage are plotted, i.e., M = 16, 64, and 256. Also plotted are the BER performances achievable by the one-tap MMSE-FDE and the matched filter (MF) bound. For comparison, the BER performance of MMSE-FDE when L = 1 is also plotted.

MMSE-FDE provides better BER performance when L = 16 than when L = 1 because of the frequency diversity effect. However, due to the residual ISI, a big performance gap from the MF bound still exists. On the other hand, iterative FD-SIC&MMSED and QRM-MLD can achieve much better BER performance than MMSE-FDE. It can be seen from Fig. 6 that as the number i of iterations increases, the BER performance of iterative FD-SIC&MMSED improves. This is because the residual ISI is effectively reduced by using the MMSE weight taking into account the residual ISI and because the error propagation can be prevented by soft ISI cancellation. It can be seen that the use of 2 iterations (i = 2) provides sufficient performance improvement. For QPSK (16QAM), the E_b/N_0 gap from the theoretical lower bound for the average BER = 10^{-4} is reduced by 1.5 (3.2) dB when i = 2. When QPSK is used, both iterative FD-SIC&MMSED and FD-QRM-MLD provide almost identical BER performance. However, when 16QAM is used, FD-QRM-MLD with either M = 64 or 256 provides better BER performance than iterative FD-SIC&MMSED.

Since this paper is to discuss the fundamental performances achievable by the frequency-domain block signal detection, we assume no channel coding. OFDM without channel coding provides BER performance similar to the SC case of L = 1 irrespective of L. As seen from Fig. 6, the SC frequency-domain block signal detection can take advantage of channel frequency-selectivity to obtain the frequency diversity gain and can achieve much better BER performance than OFDM. However, the introduction of channel coding to OFDM can significantly improve the BER performance since the channel coding across the subcarrier dimension can also take the advantage of channel frequency-selectivity. The coded OFDM can achieve slightly better BER performance than the SC transmission using MMSE-FDE as indicated in [26] (note that coded multicode DS- and MC-CDMA are considered in [26] and those with spreading factor (SF) = multiplexing order (U) = 1 correspond to coded SC and OFDM, respectively).

It should be noted that iterative FD-SIC&MMSED and FD-QRM-MLD can improve the BER performance at the cost of increased complexity compared to the MMSE-FDE and OFDM. For example, in the case of 16QAM and N_c = 64, the computational complexity (defined as the number of complex multiply operations) of iterative FD-SIC&MMSED (i = 2) and FD-QRM-MLD (M = 256) is about 4.0×10^4 times and 1.0×10^4 times higher than that of the MMSE-FDE. This is because FD-SIC&MMSED requires $(i+1)\times N_c$ times matrix inversion of an $N_c \times N_c$ matrix and QRM-MLD requires QR decomposition of an $N_c \times N_c$ matrix and a number of squared Euclidean distance calculations. Various complexity reduction algorithms for the matrix inversion have been studied [27]–[29]. We have also studied some complexity reduction schemes for FD-QRM-MLD [30], [31]. Further reducing the complexity of the proposed frequency-domain block signal detection is left as an important future study.

5. Oversampling MMSE-FDE

In most of spectrum-efficient wireless communication systems, a square-root Nyquist filter is used at the transmitter and receiver to limit the signal bandwidth while maximizing the received signal-to-noise power ratio (SNR). How-

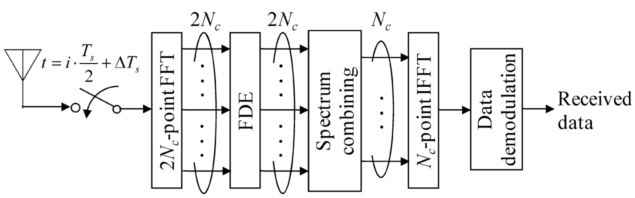

Fig. 7 Oversampling MMSE-FDE receiver.

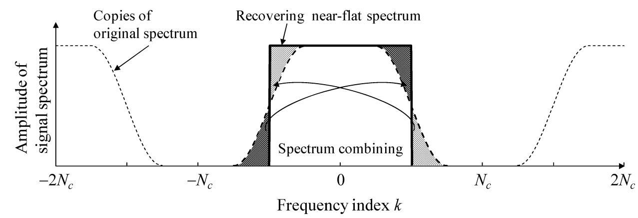

Fig. 8 Spectrum combining after one-tap MMSE-FDE.

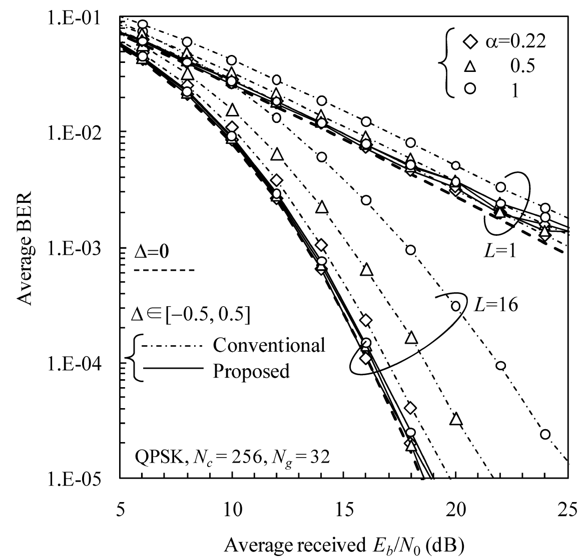

Fig. 9 BER performance in the presence of timing offset.

ever, when timing offset exists between the transmitter and receiver, the spectrum of the received signal sequence sampled at the symbol rate is distorted and hence, the BER performance degrades as the filter roll-off factor α increases. This is because adjacent frequency-shifted spectra (which are the copies of the original spectrum and are given different phase rotations due to the timing offset) overlap when $\alpha \neq 0$.

To solve the timing offset problem, recently, we proposed an oversampling MMSE-FDE [32]. Its receiver structure is illustrated in Fig. 7 (for the simplicity purpose, we omit the insertion and removal of CP). First, the received signal is oversampled at 2 times higher rate than the symbol rate to prevent the spectrum overlapping. Then, the received signal sample sequence is transformed by a $2N_c$-sample FFT into the frequency domain signal $\{R(k);\ k = -N_c \sim N_c - 1\}$. $R(k)$ can be expressed as

$$R(k) = \sqrt{\frac{2E_s}{T_s}}\tilde{H}(k,\Delta)S(k) + N(k) + \Pi(k), \tag{16}$$

where $\tilde{H}(k,\Delta)$ is the overall transfer function of the transmit plus propagation channel including the phase rotation due to the timing offset Δ, and $S(k)$, $N(k)$, and $\Pi(k)$ are the signal, the inter-block interference (IBI), and the noise, respectively.

One-tap MMSE-FDE is applied to simultaneously compensate both the phase rotation due to the timing offset and the spectrum distortion due to the channel frequency-selectivity as

$$\hat{R}(k) = R(k)W(k), \tag{17}$$

where $W(k)$ is the MMSE-FDE weight given as

$$W(k) = \frac{\tilde{H}^*(k,\Delta)}{\left|\tilde{H}(k,\Delta)\right|^2 + \Lambda^{-1}(k,\Delta)} \tag{18}$$

with $\Lambda(k,\Delta)$ being the signal-to-inter block interference plus noise power ratio (SINR), given as

$$\begin{aligned}\Lambda(k,\Delta) &= \frac{2E_s/T_s}{E[|N(k)|^2 + |\Pi(k)|^2]}\\ &= \frac{\left(\frac{E_s}{N_0}\right)}{1 + \left(\frac{E_s}{N_0}\right)\left\{\begin{array}{l}\frac{2}{N_c}\sum\limits_{l'=-\infty}^{-1}\left|h\left(\frac{l'}{2}+\Delta\right)\right|^2|l'|\\ +\frac{2}{N_c}\sum\limits_{l'=2N_g}^{\infty}\left|h\left(\frac{l'}{2}+\Delta\right)\right|^2(l'-2N_g)\end{array}\right\}}.\end{aligned} \tag{19}$$

Since $\tilde{H}(k,\Delta)$ includes the transfer function of the transmit filter, the MMSE-FDE weight also takes the role of a receive filter matched to the transmit filter (this is the reason why no receive filter is necessary in the receiver structure of Fig. 7).

After MMSE-FDE, the spectrum combing (or the frequency-domain down-sampling) is performed (see Fig. 8) to restore the ISI-free condition (note that the perfect restoration of the ISI-free condition cannot be achieved in the frequency-selective channel case) as

$$\tilde{R}(k) = \hat{R}(k - N_c) + \hat{R}(k) + \hat{R}(k + N_c) \tag{20}$$

for $k = -N_c/2 \sim N_c/2 - 1$. After spectrum combining, an N_c-point inverse FFT (IFFT) is applied to the frequency-domain signal $\{\tilde{R}(k);\ k = -N_c/2 \sim N_c/2 - 1\}$ for succeeding data demodulation.

The BER performances of the proposed oversampling MMSE-FDE and of the conventional symbol rate sampling MMSE-FDE are compared for the frequency-selective Rayleigh fading channel having $L = 16$-path uniform power delay profile and the frequency-nonselective Rayleigh fading channel ($L = 1$), respectively. It is seen from Fig. 9 that the proposed oversampling MMSE-FDE provides a good BER performance which is insensitive to α in the presence of the timing offset regardless of the degree of the channel frequency-selectivity.

6. Joint Transmit/Receive MMSE-FDE

If the channel state information (CSI) is available at the transmitter, transmit FDE (or called pre-FDE) can be jointly used with the receive FDE to compensate the signal spectrum distortion due to the channel frequency-selectivity. The frequency-domain representation of the transmission system using joint transmit/receive MMSE-FDE is illustrated in Fig. 10 (for the simplicity purpose, we omit the insertion and removal of CP).

Before transmitting the signal, an N_c-symbol block $\boldsymbol{d}$ is transformed by an N_c-point FFT into a frequency-domain signal block $\boldsymbol{D} = \boldsymbol{Fd}$. One-tap transmit FDE weight is multiplied to each element (frequency component) of $\boldsymbol{D}$. Denoting an $N_c \times N_c$ transmit FDE weight matrix by $\boldsymbol{W}_t = diag\{W_t(0), \ldots, W_t(k), \ldots, W_t(N_c-1)\}$, the time-domain signal block $\boldsymbol{s}$ after carrying out N_c-point IFFT can be expressed as

$$\boldsymbol{s} = C \cdot \boldsymbol{F}^H \boldsymbol{W}_t \boldsymbol{F} \boldsymbol{d}, \tag{21}$$

where $C = \sqrt{N_c / tr[\boldsymbol{W}_t \boldsymbol{W}_t^H]}$ is the transmit power normalization coefficient. After transforming the frequency-domain signal block by an N_c-point IFFT into the time-domain transmit signal block, the signal block is transmitted.

The received signal block is transformed into frequency-domain signal block $\boldsymbol{R} = [R(0), \ldots, R(k), \ldots, R(N_c-1)]^T$ by N_c-point FFT as

$$\boldsymbol{R} = \boldsymbol{F}\left(\sqrt{\frac{2E_s}{T_s}}\boldsymbol{hs} + \boldsymbol{n}\right) = \sqrt{\frac{2E_s}{T_s}}\left(\boldsymbol{FhF}^H\right)(\boldsymbol{Fs}) + \boldsymbol{Fn}$$
$$= \sqrt{\frac{2E_s}{T_s}} C \cdot \boldsymbol{HW}_t \boldsymbol{Fd} + \boldsymbol{N}. \tag{22}$$

At the receiver, one-tap receive FDE is carried out and then, N_c-point IFFT is performed to transform the frequency-domain signal block back into the decision variable block $\hat{\boldsymbol{d}}$. Denoting an $N_c \times N_c$ receive FDE weight matrix by $\boldsymbol{W}_r = diag\{W_r(0), \ldots, W_r(k), \ldots, W_r(N_c-1)\}$, $\hat{\boldsymbol{d}}$ is expressed as

$$\hat{\boldsymbol{d}} = \boldsymbol{F}^H \boldsymbol{W}_r \boldsymbol{R} = \sqrt{\frac{2E_s}{T_s}} C \cdot \boldsymbol{F}^H (\boldsymbol{W}_r \boldsymbol{HW}_t) \boldsymbol{Fd} + \boldsymbol{F}^H \boldsymbol{W}_r \boldsymbol{N}. \tag{23}$$

In the case of MC transmission (e.g., OFDM), the decision variable block $\hat{\boldsymbol{d}}_{MC}$ is expressed as

$$\hat{\boldsymbol{d}}_{MC} = \sqrt{\frac{2E_s}{T_s}} C \cdot (\boldsymbol{W}_r \boldsymbol{HW}_t)\, \boldsymbol{d} + \boldsymbol{W}_r \boldsymbol{N}. \tag{24}$$

It can be understood from Eqs. (23) and (24) that the use of transmit and receive FDE transforms the channel $\boldsymbol{H}$ into an equivalent channel $\boldsymbol{W}_r \boldsymbol{HW}_t$ for both SC and MC (note that $\boldsymbol{W}_t$ and $\boldsymbol{W}_r$ can be generalized to include spreading and de-spreading). Therefore, $\boldsymbol{W}_t$ and $\boldsymbol{W}_r$ can be optimized regardless of transmit signal waveforms (i.e., SC and MC). For example, the choice of waveforms can be made based on the peak-to-average power ratio (PAPR).

If $\boldsymbol{W}_t$ and $\boldsymbol{W}_r$ are chosen so as to satisfy $\boldsymbol{W}_r \boldsymbol{HW}_t = \boldsymbol{I}$, the channel frequency-selectivity problem can be completely removed. However, since most of the transmit power is allocated to the frequencies with lower channel gains, less power is allocated to other frequencies in order to keep the transmit power the same. Therefore, the received signal power is significantly reduced, thereby significantly degrading the BER performance. In [33], we proposed the joint transmit/receive MMSE-FDE for SC transmissions. Since it is quite difficult to find the exact MMSE solution of ($\boldsymbol{W}_t$, $\boldsymbol{W}_r$), we took a sub-optimal approach: $\boldsymbol{W}_r$ is derived first for the given $\boldsymbol{W}_t$ and then, $\boldsymbol{W}_t$ is derived assuming that the derived $\boldsymbol{W}_r$ is used. By treating the concatenation $\boldsymbol{HW}_t$ of the transmit FDE and channel as an equivalent channel, $\boldsymbol{W}_r$ is given as

$$\boldsymbol{W}_r = \boldsymbol{W}_t^H \boldsymbol{H}^H [\boldsymbol{HW}_t \boldsymbol{W}_t^H \boldsymbol{H}^H + C^{-1}\gamma^{-1} \cdot \boldsymbol{I}]^{-1}, \tag{25}$$

where $\gamma = (E_s/N_0)$. Then, $\boldsymbol{W}_t$ is derived as [27]

$$\boldsymbol{W}_t = diag\{|W_t(0)|, \ldots, |W_t(k)|, \ \ldots, |W_t(N_c-1)|\} \tag{26}$$

with

$$|W_t(k)|^2 = \max\left[\frac{1}{\mu}\frac{1}{\sqrt{\gamma}|H(k)|} - \frac{1}{\gamma|H(k)|^2}, 0\right], \tag{27}$$

where μ is the constant which satisfies $tr[\boldsymbol{W}_t \boldsymbol{W}_t^H] = N_c$.

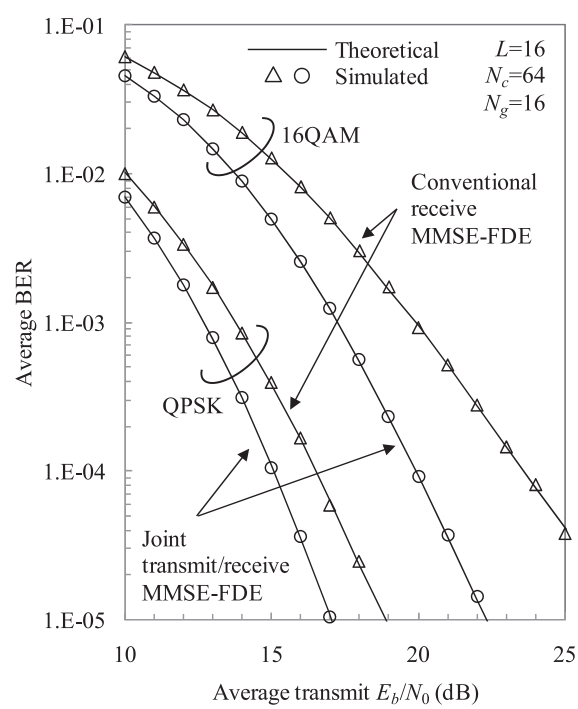

Fig. 11 BER performance of SC using the joint transmit/receive MMSE-FDE.

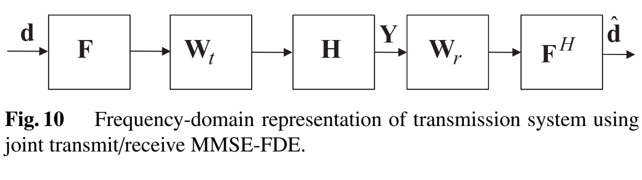

Fig. 10 Frequency-domain representation of transmission system using joint transmit/receive MMSE-FDE.

Figure 11 plots the achievable BER performance of SC using the joint transmit/receive MMSE-FDE. For comparison, the BER performance of SC using the conventional receive MMSE-FDE is also plotted. It can be seen from Fig. 11 that the joint transmit/receive MMSE-FDE provides much better BER performance than the conventional receive MMSE-FDE.

One of remaining problems for implementing the joint transmit/receive MMSE-FDE is to estimate the CSI at the transmitter side. Many studies for estimating the CSI at the transmitter can be found [34]–[37]. How the proposed joint transmit/receive MMSE-FDE is sensitive to the CSI error is an important future study topic.

7. Distributed Antenna Network

In DAN, many antennas are spatially distributed around a BS so that with a high probability, there are some distributed antennas in the vicinity of an MT. Distributed antennas are connected to a SPC by means of optical fiber or wireless links, as illustrated in Fig. 12. They can cooperate to perform spatial diversity, beam forming, or spatial multiplexing. The distributed antenna spatial diversity can mitigate the received signal power loss problem caused by distance-dependent path loss and shadowing loss as well as the frequency-selective fading.

One of promising distributed antenna diversity for DAN downlink is MRT [38] that exploits the CSI at the network transmitter side. In a frequency-selective channel, MRT is incorporated into the transmit FDE. This is called MRT-FDE. As seen in Fig. 13, the signal block is simultaneously transmitted from N_t distributed antennas in the vicinity of an MT after multiplying MRT-FDE weight $\{W_m(k);\ k = 0{\sim}N_c - 1\}$, $m = 0{\sim}N_t - 1$, so that the same frequency components transmitted from N_t distributed antennas are coherently combined at the MT, where N_t is the number of distributed antennas involved in MRT-FDE.

The signal block $\boldsymbol{s}$ transmitted from N_t distributed antennas can be expressed using the matrix form as

$$\begin{aligned}\boldsymbol{s} &= [\boldsymbol{s}_0, \cdots, \boldsymbol{s}_m, \cdots, \boldsymbol{s}_{N_t-1}]^T \\ &= \left[\left(\boldsymbol{F}^H\boldsymbol{W}_0\boldsymbol{F}\right)\boldsymbol{d}, \cdots, \left(\boldsymbol{F}^H\boldsymbol{W}_m\boldsymbol{F}\right)\boldsymbol{d}, \cdots, \left(\boldsymbol{F}^H\boldsymbol{W}_{N_t-1}\boldsymbol{F}\right)\boldsymbol{d}\right]^T.\end{aligned} \tag{28}$$

where $\boldsymbol{W}_m = \mathrm{diag}\{W_m(0), \cdots, W_m(k), \cdots, W_m(N_c - 1)\}$ is the MRT-FDE weight matrix associated with the mth antenna, given by

$$\boldsymbol{W}_m = \left(\frac{1}{N_c}\sum_{m'=0}^{N_t-1}\sum_{k'=0}^{N_c-1}\left|H_{m'}(k')\right|^2\right)^{-\frac{1}{2}}\boldsymbol{H}_m^*, \tag{29}$$

where $\boldsymbol{H}_m = \boldsymbol{F}\boldsymbol{h}_m\boldsymbol{F}^H$ is given by

$$\begin{aligned}\boldsymbol{H}_m &= \boldsymbol{F}\boldsymbol{h}_m\boldsymbol{F}^H \\ &= \begin{bmatrix} H_m(0) & & & & \\ & \ddots & & \boldsymbol{0} & \\ & & H_m(k) & & \\ & \boldsymbol{0} & & \ddots & \\ & & & & H_m(N_c-1) \end{bmatrix}.\end{aligned} \tag{30}$$

The received signal block $\boldsymbol{r} = [r(0), \cdots, r(t), \cdots, r(N_c-1)]^T$ at an MT can be expressed as

$$\boldsymbol{r} = \sqrt{\frac{2E_s}{T_s}}\boldsymbol{h}\boldsymbol{s} + \boldsymbol{n}, \tag{31}$$

where $\boldsymbol{h} = [\boldsymbol{h}_0, \cdots, \boldsymbol{h}_m, \cdots, \boldsymbol{h}_{N_t-1}]$, $\boldsymbol{h}_m$ is the channel impulse response matrix of size $N_c \times N_c$ associated with the mth antenna, given as

$$\boldsymbol{h}_m = \begin{bmatrix} h_{m,0} & & & & h_{m,L-1} & \cdots & h_{m,1} \\ h_{m,1} & \ddots & & & & \ddots & \vdots \\ \vdots & \ddots & h_{m,0} & & \boldsymbol{0} & & h_{m,L-1} \\ h_{m,L-1} & & h_{m,1} & \ddots & & & \\ & \ddots & \vdots & \ddots\ \ddots & & & \\ & & h_{m,L-1} & \ddots & h_{m,0} & & \\ & & & \ddots & h_{m,1} & \ddots & \\ \boldsymbol{0} & & & \ddots & \vdots & \ddots & h_{m,0} \end{bmatrix}, \tag{32}$$

and $\boldsymbol{n} = [n(0), \cdots, n(t), \cdots, n(N_c - 1)]^T$ is the noise vector.

The frequency-domain representation $\boldsymbol{R}$ of the received signal block is given as

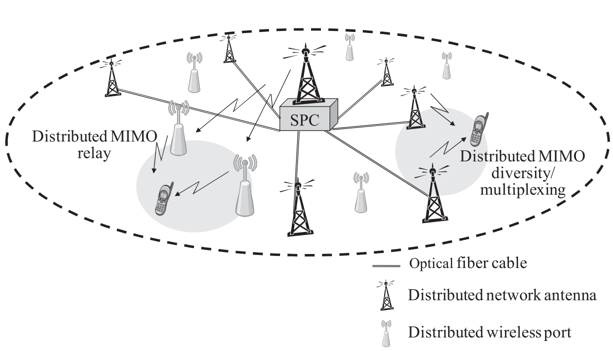

Fig. 12 Distributed antenna network.

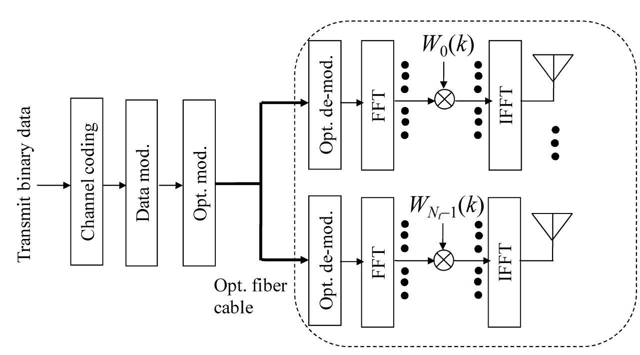

Fig. 13 DAN downlink using SC MRT-FDE.

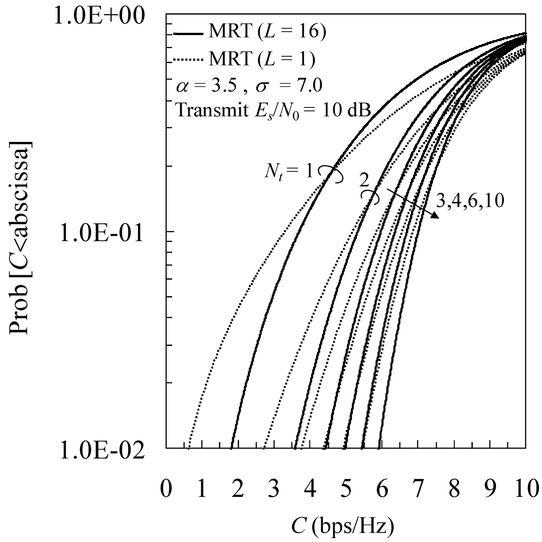

Fig. 14 Channel capacity distribution of distributed antenna diversity using SC MRT-FDE.

$$\boldsymbol{R} = \boldsymbol{F}\boldsymbol{r} = \sqrt{\frac{2E_s}{T_s}}\left(\sum_{m=0}^{N_t-1}\boldsymbol{H}_m\boldsymbol{W}_m\right)\boldsymbol{F}\boldsymbol{d} + \boldsymbol{N}, \qquad (33)$$

where $\boldsymbol{N} = \boldsymbol{F}\boldsymbol{n}$.

The MRT-FDE maximizes the received SNR at each frequency k, but enhances the ISI in the case of SC transmissions. Therefore, the ISI cancellation is necessary in the signal detection.

Similar to Eq. (8), the channel capacity C of SC DAN using MRT-FDE is given, from Eq. (33), as

$$\begin{aligned} C &= \frac{1}{N_c}\log_2 \det\left(\boldsymbol{I} + \frac{E_s}{N_0}\left(\sum_{m=0}^{N_t-1}\boldsymbol{H}_m\boldsymbol{W}_m\right)\left(\sum_{m=0}^{N_t-1}\boldsymbol{H}_m\boldsymbol{W}_m\right)^H\right) \\ &= \frac{1}{N_c}\sum_{k=0}^{N_c-1}\log_2\left(1 + \frac{E_s}{N_0}\frac{\left(\sum_{m=0}^{N_t-1}|H_m(k)|^2\right)^2}{\frac{1}{N_c}\sum_{m=0}^{N_t-1}\sum_{k'=0}^{N_c-1}|H_m(k')|^2}\right). \end{aligned} \qquad (34)$$

The channel capacity changes according to the movement of an MT because of the frequency-selective fading, shadowing loss, and distant-dependent path loss. The channel capacity distribution of SC MRT-FDE is plotted in Fig. 14. Due to higher frequency diversity gain, the 1% outage channel capacity when $L = 16$ is higher than that when $L = 1$.

Another approach is the use of distributed antennas as relay nodes. Multiple relay nodes in the vicinity of an MT cooperate to relay the signal transmitted from the MT to a SPC. Multiple relay nodes can perform the antenna beam forming or MRT-FDE to improve the SC signal transmission performance. Note that in the case of OFDM, adaptive subcarrier allocation over multiple 2-hop routes constructed by relay nodes can be introduced to make use of the frequency and spatial diversity [39].

8. Conclusions

This article introduced the recent advances in FDE and DAN for the broadband SC signal transmissions. To realize the high quality broadband SC signal transmissions, there are two crucial issues to overcome: the channel frequency-selectivity and the power loss due to the shadowing and distance-dependant path losses. The frequency-domain block signal detection that incorporates the idea of MIMO signal detection into FDE to effectively suppress the ISI was introduced. In addition, the oversampling one-tap MMSE-FDE that can mitigate the problem arising from the timing offset between the transmitter and receiver was introduced. Finally, DAN was presented that can mitigate the received signal power loss problem caused by distance-dependent path loss and shadowing loss while exploiting the frequency-selective fading.

References

[1] Y. Kim, B.J. Jeong, J. Chung, C.-S. Hwang, J.S. Ryu, K.-H. Kim, and Y.J. Kim, "Beyond 3G; vision, requirements, and enabling technologies," IEEE Commun. Mag., vol.41, no.3, pp.120–124, March 2003.

[2] J.G. Proakis, Digital communications, 4th ed., McGraw-Hill, 2001.

[3] D. Falconer, S.L. Ariyavistakul, A. Benyamin-Seeyar, and B. Eidson, "Frequency domain equalization for single-carrier broadband wireless systems," IEEE Commun. Mag., vol.40, no.4, pp.58–66, April 2002.

[4] F. Adachi, T. Sao, and T. Itagaki, "Performance of multicode DS-CDMA using frequency domain equalization in a frequency selective fading channel," Electron. Lett., vol.39, no.2, pp.239–241, Jan. 2003.

[5] A.S. Madhukumar, F. Chin, Y.-C. Liang, and K. Yang, "Single-carrier cyclic prefix-assisted CDMA system with frequency domain equalization for high data rate transmission," EURASIP J. Wireless Communications and Networking, vol.2004, no.1, pp.149–160, Aug. 2004.

[6] F. Adachi, D. Garg, S. Takaoka, and K. Takeda, "Broadband CDMA techniques," IEEE Wireless Commun. Mag., vol.12, no.2, pp.8–18, April 2005.

[7] F. Adachi, K. Takeda, and H. Tomeba, "Frequency-domain equalization for broadband single-carrier multiple access," IEICE Trans. Commun., vol.E92-B, no.5, pp.1441–1456, May 2009.

[8] T. Yamamoto, K. Takeda, and F. Adachi, "A study of frequency-domain signal detection for single-carrier transmission," 2009 IEEE 70th Vehicular Technology Conference (VTC2009-Fall), Anchorage, Alaska, USA, Sept. 2009.

[9] S. Liu, Z. He, and W. Wu, "Transmit diversity method with user's power constraint for distributed antenna system," Proc. 2nd International Symposium on Wireless Pervasive Computing (ISWPC'07), San Juan, Puerto Rico, Feb. 2007.

[10] A.M. Saleh, A.J. Rustako, and R.S. Roman, "Distributed antennas for indoor radio communications," IEEE Trans. Commun., vol.CON-35, no.12, pp.1245–1251, Dec. 1987.

[11] M.V. Clark, T.M. Willes III, L.J. Greenstein, A.J. Rustako, Jr., V. Erceg, and R.S. Roman, "Distributed versus centralized antenna arrays in broadband wireless networks," Proc. IEEE Veh. Technol. Conf. (VTC2001-Spring), pp.33–37, Rhodes, Greece, May 2001.

[12] L. Dai, S. Zho, and Y. Yao, "Capacity analysis in CDMA distributed antenna systems," IEEE Trans. Wireless Commun., vol.4, no.6, pp.2613–2620, Nov. 2006.

[13] W. Choi, “Downlink performance and capacity of distributed antenna systems in a multicell environment,” IEEE Trans. Wireless Commun., vol.6, no.1, pp.69–73, Jan. 2007.
[14] H. Matsuda, H. Tomeba, and F. Adachi, “Channel capacity of distributed antenna system using maximal ratio transmission,” 5th IEEE VTS Asia Pacific Wireless Communications Symposium (APWCS2008), Sendai, Japan, Aug. 2008.
[15] T.S. Rappaport, Wireless communications, Prentice Hall, 1996.
[16] J. Louveaux, L. Vandendorpe, and T. Sartenaer, “Cyclic prefixed single carrier and multicarrier transmission: Bit rate comparison,” IEEE Commun. Lett., vol.7, no.4, pp.180–182, April 2003.
[17] G.J. Foschini and M.J. Gans, “On limits of wireless communications in a fading environment when using multiple antennas,” Wirel. Pers. Commun., vol.6, no.3, pp.311–335, March 1998.
[18] H. Bolcskei, D. Gesbert, and A.J. Paulraj, “On the capacity of OFDM-based spatial multiplexing systems,” IEEE Trans. Commun., vol.50, no.2, pp.225–234, Feb. 2002.
[19] P.W. Wolniansky, G.J. Foschini, G.D. Golden, and R.A. Valenzuela, “V-BLAST: An architecture for realizing very high data rates over the rich-scattering wireless channel,” Proc. 1998 URSI International Symposium on Signals, Systems, and Electronics (ISSSE’98), pp.295–300, Pisa, Italy, Sept.-Oct. 1998.
[20] L.J. Kim and J. Yue, “Joint channel estimation and data detection algorithms for MIMO-OFDM systems,” Proc. Thirty-Sixth Asilomar Conference on Signals, System and Computers, pp.1857–1861, Pacific Grove, CA, U.S.A., Nov. 2002.
[21] R. Bohnke and K. Kammeyer, “SINR analysis for V-BLAST with ordered MMSE-SIC detection,” Proc. International Wireless Communications and Mobile Computing Conference, pp.623–628, Vancouver, Canada, July 2006.
[22] C. Shen, H. Zhuang, L. Dai, S. Zhou, and Y. Yao, “Performance improvement of V-BLAST through an iterative approach,” Proc. IEEE Personal, Indoor and Mobile Radio Communications Symposium (PIMRC’03), vol.3, pp.2553–2557, Beijing, China, Sept. 2003.
[23] A. Nakajima and F. Adachi, “Iterative FDIC using 2D-MMSE FDE for turbo-coded HARQ in SC-MIMO multiplexing,” IEICE Trans. Commun., vol.E90-B, no.3, pp.693–695, March 2007.
[24] F. Adachi, K. Takeda, and Y. Kojima, “On computation of mean squared equalization error for single-carrier iterative frequency-domain equalization & residual interference cancellation,” Proc. IEICE Gen. Conf. 2009, BS-3-14, March 2009.
[25] B. Anderson and S. Mohan, “Sequential coding algorithms: A survey and cost analysis,” IEEE Trans. Commun., vol.CON-32, pp.169–176, Feb. 1984.
[26] F. Adachi, A. Nakajima, K. Takeda, L. Liu, H. Tomeba, T. Yui, and K. Fukuda, “Frequency-domain equalization for block CDMA transmission,” European Trans. Telecommunications (ETT), vol.19, no.5, pp.553–560, June 2008.
[27] C.R. Glassey, “An orthogonalization method of computing the generalized inverse of matrix,” ORC-66-10, Operations Research Center, Univ. of California, Berkeley, 1966.
[28] T.N.E. Grevill, “Some applications of the pseudo inverse of a matrix,” SIAM Review, vol.2, no.1, pp.15–22, Jan. 1960.
[29] A. Ben-Israel and S.J. Wersasn, “An elimination method for computing the generalized inverse of an arbitrary complex matrix,” J. ACM, vol.10, pp.532–537, Oct. 1963.
[30] T. Yamamoto, K. Takeda, and F. Adachi, “Training sequence aided single-carrier block signal detection using QRM-MLD,” Proc. IEEE Wireless Communication & Networking Conference (WCNC), Sydney, Australia, April 2010.
[31] T. Yamamoto, K. Takeda, and F. Adachi, “MMSE based QRM-MLD Frequency-domain block signal detection for single-carrier transmission,” 7th IEEE VTS Asia Pacific Wireless Communication Symposium (APWCS 2010), Kaohsiung, Taiwan, May 2010.
[32] T. Obara, K. Takeda, and F. Adachi, “Oversampling frequency-domain equalization for single-carrier transmission in the presence of timing offset,” 6th IEEE VTS Asia Pacific Wireless Communications Symposium (APWCS’09), Seoul, Korea, Aug. 2009.
[33] K. Takeda, H. Tomeba, and F. Adachi, “Multicode DS-CDMA using joint transmit/receive MMSE-FDE,” Proc. IEEE Personal, Indoor and Mobile Radio Communications Symposium (PIMRC’09), Tokyo, Japan, Sept. 2009.
[34] Y. Zhu and K.B. Letaief, “Frequency domain pre-equalization with transmit precoding for MIMO broadband wireless channels,” J. Sel. Areas Commun., vol.26, no.2, pp.389–400, 2008.
[35] L. Sanquinetti, I. Cosovic, and M. Morelli, “Channel estimation for MC-CDMA uplink transmissions with combined equalization,” J. Sel. Areas Commun., vol.24, no.6, pp.1167–1178, 2006.
[36] D. Tsipouridou and A.P. Liavas, “On the sensitivity of transmit MIMO wiener filter with respect to channel and noise second-order statistics uncertainties,” IEEE Trans. Signal Process., vol.56, no.2, pp.832–838, 2008.
[37] N. Lynn, K. Adachi, O. Takyu, and M. Nakagawa, “Effect of channel mismatch on AMC in asymmetric TDD/OFDM system with pre-equalization downlink,” Proc. Information Theory and Its Applications (ISITA), Auckland, New Zealand, Dec. 2008.
[38] J.K. Cavers, “Single-user and multiuser adaptive maximal ratio transmission for Rayleigh channels,” IEEE Trans. Veh. Technol., vol.49, no.6, pp.2043–2050, Nov. 2000.
[39] H. Ishida, E. Kudoh, and F. Adachi, “Channel capacity of parallel relaying 2-hop OFDMA virtual cellular network,” Proc. IEEE 70th Vehicular Technology Conference (VTC’09-Fall), Anchorage, Alaska, USA, Sept. 2009.

Fumiyuki Adachi received the B.S. and Dr.Eng. degrees in electrical engineering from Tohoku University, Sendai, Japan, in 1973 and 1984, respectively. In April 1973, he joined the Electrical Communications Laboratories of Nippon Telegraph & Telephone Corporation (now NTT) and conducted various types of research related to digital cellular mobile communications. From July 1992 to December 1999, he was with NTT Mobile Communications Network, Inc. (now NTT DoCoMo, Inc.), where he led a research group on wideband/broadband CDMA wireless access for IMT-2000 and beyond. Since January 2000, he has been with Tohoku University, Sendai, Japan, where he is a Professor of Electrical and Communication Engineering at the Graduate School of Engineering. His research interests are in CDMA wireless access techniques, equalization, transmit/receive antenna diversity, MIMO, adaptive transmission, and channel coding, with particular application to broadband wireless communications systems. He is a program leader of the 5-year Global COE Program “Center of Education and Research for Information Electronics Systems” (2007–2011), awarded by the Ministry of Education, Culture, Sports, Science and Technology of Japan. From October 1984 to September 1985, he was a United Kingdom SERC Visiting Research Fellow in the Department of Electrical Engineering and Electronics at Liverpool University. He is an IEICE Fellow and was a co-recipient of the IEICE Transactions best paper of the year award 1996, 1998, and 2009 and also a recipient of Achievement award 2003. He is an IEEE Fellow and was a co-recipient of the IEEE Vehicular Technology Transactions best paper of the year award 1980 and again 1990 and also a recipient of Avant Garde award 2000. He was a recipient of Thomson Scientific Research Front Award 2004, Ericsson Telecommunications Award 2008, and Telecom System Technology Award 2010.

Kazuki Takeda received his B.S. and M.S. degree in communications engineering from Tohoku University, Sendai, Japan, in 2006 and 2008. Currently he is a Japan Society for the Promotion of Science (JSPS) research fellow, studying toward his Ph.D. degree at the Department of Electrical and Communications Engineering, Graduate School of Engineering, Tohoku University. His research interests include precoding and channel equalization techniques for mobile communication systems. He was a recipient of the 2010 IEICE RCS (Radio Communication Systems) Active Research Award.

Tatsunori Obara received his B.S. degree in Electrical, Information and Physics Engineering in 2008 and M.S. degree in communications engineering, in 2010, respectively, from Tohoku University, Sendai Japan. Currently he is a graduate student, studying toward his Ph.D. degree at the Department of Electrical and Communications Engineering, Graduate School of Engineering, Tohoku University. His research interests include channel equalization techniques for mobile communication systems.

Tetsuya Yamamoto received his B.S. degree in Electrical, Information and Physics Engineering in 2008 and M.S. degree in communications engineering, in 2010, respectively, from Tohoku University, Sendai Japan. Currently he is a Japan Society for the Promotion of Science (JSPS) research fellow, studying toward his Ph.D. degree at the Department of Electrical and Communications Engineering, Graduate School of Engineering, Tohoku University. His research interests include frequency-domain equalization and signal detection techniques for mobile communication systems. He was a recipient of the 2009 IEICE RCS (Radio Communication Systems) Active Research Award.

Hiroki Matsuda received his B.S. degree in Electrical, Information and Physics Engineering in 2008 and M.S. degree in communications engineering, in 2010, respectively, from Tohoku University, Sendai Japan. Since April 2010, he has been with Sony Corporation. His research interests include antenna diversity techniques for distributed antenna network.